Chaos ARTICLE pubs.aip.org/aip/cha

# Parametric modeling of mechanical effects on circadian oscillators

Cite as: Chaos 34, 013135 (2024); doi: 10.1063/5.0164829
Submitted: 24 June 2023 · Accepted: 19 December 2023 ·
Published Online: 23 January 2024



Keith E. Kennedy,[1] Juan F. Abenza,[2] Leone Rossetti,[2] Xavier Trepat,[2,3,4,5] Pablo Villoslada,[1,6] and Jordi Garcia-Ojalvo[1,a)]

## AFFILIATIONS

[1]Department of Medicine and Life Sciences, Universitat Pompeu Fabra, Barcelona Biomedical Research Park, 08003 Barcelona, Spain
[2]Institute for Bioengineering of Catalonia, Barcelona Institute for Science and Technology, 08028 Barcelona, Spain
[3]Facultat de Medicina, Universitat de Barcelona, 08036 Barcelona, Spain
[4]Institució Catalana de Recerca i Estudis Avançats, 08010 Barcelona, Spain
[5]Centro de Investigación Biomédica en Red en Bioingeniería, Biomateriales y Nanomedicina (CIBER-BBN), 08028 Barcelona, Spain
[6]Hospital del Mar Medical Research Institute, Barcelona Biomedical Research Park, 08003 Barcelona, Spain

**Note:** This paper is part of the Focus Issue on Nonlinear dynamics, synchronization and networks: Dedicated to Juergen Kurths' 70th birthday.

[a)]**Author to whom correspondence should be addressed:** jordi.g.ojalvo@upf.edu

## ABSTRACT

Circadian rhythms are archetypal examples of nonlinear oscillations. While these oscillations are usually attributed to circuits of biochemical interactions among clock genes and proteins, recent experimental studies reveal that they are also affected by the cell's mechanical environment. Here, we extend a standard biochemical model of circadian rhythmicity to include mechanical effects in a parametric manner. Using experimental observations to constrain the model, we suggest specific ways in which the mechanical signal might affect the clock. Additionally, a bifurcation analysis of the system predicts that these mechanical signals need to be within an optimal range for circadian oscillations to occur.





**Cells are nonlinear dynamical elements, which in multicellular tissues are commonly coupled to one another. Much work has been done, both theoretically and experimentally, to understand this coupling and to identify its dynamical consequences from a biochemical viewpoint. In contrast, much less is known about how the mechanical interactions between cells affect these dynamics. Recent work has shown, for instance, that circadian oscillations degrade substantially in populations of cells *in vitro* when cell density decreases sufficiently. Here, we use this fact to constrain a standard model of circadian oscillations and propose a way through which external mechanical signals and internal biochemical interactions could combine in clock cells.**

## I. INTRODUCTION

Molecular clocks are present in all organisms on Earth, ranging from bacteria to humans.[1] One of these clocks is the circadian day/night rhythm, whose intrinsic period is around 24 h.[2,3] Adhering to this clock is crucial for survival, as organisms need to behave differently in the presence or absence of daylight, in order to thrive in natural ecosystems.[4]

In multicellular organisms, cells need to synchronize their circadian rhythms across and between tissues.[5,6] The general conditions underlying the synchronization of nonlinear systems (of which circadian oscillators are an example) were explored by Arthur Winfree and others as far back as the 1960s[7–9] and described in further detail by Jürgen Kurths and others over the 1990s and 2000s.[10–12] In the case of circadian clocks, rhythm coordination can arise from biochemical signaling, mechanical interactions, or (most likely) through a combination of both. While much effort has been devoted to studying the biochemical aspects of circadian cell–cell coordination,[13–18] the role of mechanical interactions on circadian rhythmicity is still largely unexplored.

Here, we address this question by including mechanical factors in a biochemical model based on a standard architecture for genetic oscillations. The model represents mechanical effects through the activity of the transcription factors YAP/TAZ, which are known to sense mechanical signals.[19] Changes in the cell's microenvironment due to phenomena such as apoptosis, proliferation, and motion of neighboring cells affect the nuclear localization of these proteins, thereby altering their transcriptional regulatory activity.[19,20] Recent experimental observations have revealed that the levels of YAP/TAZ signaling, controlled either through changes in cell density or directly through overexpression, determine the quality of circadian rhythms (in terms of period stability) in mouse fibroblasts.[21] We use this observation and the measured effects of YAP/TAZ on the clock gene Rev-Erbα to constrain our model and to suggest a potential mechanism through which these mechanical effects may arise.

## II. EXPERIMENTAL CONSTRAINTS

Circadian oscillations are possible thanks to well-structured biochemical networks. In mammals, the genes at the heart of the clock include the activators Clock and Bmal as well as the transcriptional repressors Per and Cry. Clock and Bmal form a complex that activates the expression of Per and Cry, which bind to each other in the cytoplasm and return to the nucleus to inhibit their own expression. This leads to a nonlinear transcription-translation negative feedback loop that is capable of sustaining oscillations in gene expression.[3] A second feedback is provided by the nuclear receptor Rev-Erbα, whose transcription is also activated by the Clock/Bmal complex and inhibits Bmal itself upon returning to the nucleus, forming an additional negative feedback loop that adds robustness to the core network.[22,23]

Recent experiments in mouse fibroblasts[21] have shown that Rev-Erbα is cell-density dependent, which results in circadian rhythms being more robust for higher cell densities. A representative realization of those experimental results is shown in Fig. 1(a). This behavior has physiological consequences: during wound healing, for instance, circadian robustness is lost as the cells on the wound front have lower cell density.[21] The molecular connection between cell–cell contact and the molecular clock is believed to be mediated by YAP and TAZ, whose concentrations are known to decrease with increasing cell density.[24] In agreement with this fact, overexpression of TAZ leads to a disappearance of circadian rhythmicity, as shown in Fig. 1(b) (blue line). This contrasts with the behavior exhibited by the cells in basal conditions, for which a clear spectral peak at a period of 1 day is observed [red line in Fig. 1(b)]. That circadian peak is completely absent for the case of TAZ overexpression, which corresponds to low cell densities in the experiments shown in Fig. 1(a). Additionally, experiments show that TAZ overexpression leads to increased Rev-Erbα levels [Fig. 1(c)].

## III. MODELING THE CIRCADIAN EFFECTS OF YAP/TAZ

The molecular mechanism through which increased YAP/TAZ nuclear concentration (and correspondingly low cell density) causes cells to lose their circadian rhythmicity remains unknown. In what follows, we address this question using a variation in the Goodwin model to simulate the effect of YAP/TAZ on the robustness of the circadian clock. Our model aims to propose a specific mechanism by which YAP/TAZ can affect the quality of circadian oscillations. Furthermore, the model aims to predict possible outcomes that were not tested in previous experiments, such as the effect of decreasing YAP/TAZ levels (and correspondingly increasing cell density). Also, it will help us to better understand how the system responds to continuous changes in YAP/TAZ levels: Do cells lose the oscillations suddenly at a certain concentration of YAP/TAZ, or do the oscillations gradually fade away?

The model aims to simplify as much as possible the interactions among the molecular species present in the system, keeping only the elements of the clock that are essential for rhythm generation. We constrain the model using the experimental observations described above, together with scaling information such as the period of oscillation and typical molecule levels of the clock components.

The Goodwin model[25] is commonly used to describe the dynamics of circadian oscillators.[26,27] It consists of three coupled ordinary differential equations describing the dynamics of three biochemical components connected to one another in a negative feedback loop,

$$\frac{dX}{dt} = \frac{\alpha_1}{1 + \left(\frac{Z}{K}\right)^h} - d_1 X, \tag{1}$$

$$\frac{dY}{dt} = \beta_2 X - d_2 Y, \tag{2}$$

$$\frac{dZ}{dt} = \beta_3 Y - \frac{d_3 Z}{1 + \frac{Z}{S}}. \tag{3}$$

Here, $\alpha_1$ is the maximum expression of $X$, $K$ is the negative feedback strength of $Z$ on $X$, $h$ is the Hill coefficient, $\beta_2$ and $\beta_3$ are production rates, and $d_1$, $d_2$, and $d_3$ are decay rates. This model can be used to simulate the expression levels of a simplified version of the molecular clock network, in which only the feedback loop among Bmal mRNA (represented by $X$ above), Rev-Erbα mRNA ($Y$), and Rev-Erbα protein ($Z$) is considered.[27]

An advantage of the Goodwin model is its simplicity and well-documented use. However, the equations must be adjusted to realistically represent a circadian clock. First, the model parameters must be properly selected to reflect known concentrations of molecules within a cell and to produce a period on the order of 24 h. This can be done by rescaling the model variables (concentrations and time) as usually done in dimensional analysis[27] and selecting the scaling factors that lead to the correct ranges in the values of the variables. These factors also rescale the model parameters: applying the scaling factors obtained above to the parameters of Ananthasubramaniam *et al.*[27] led us to the parameter values given in Table I. These parameters produce oscillations with biologically realistic period and amplitude ranges,[28] as shown in Fig. 2. The code for the model simulation and subsequent analysis is available at https://github.com/dsb-lab/mech-gene-clock.

Additionally, saturation was added to the decay term of Rev-Erbα protein ($Z$) in Eq. (3) to increase the modulation depth of the oscillations of that variable, which was too small when using the standard parameter set in the common version of the model with linear saturation.[27] The modulation depth is defined as the amplitude of the oscillations divided by their mean and provides an idea

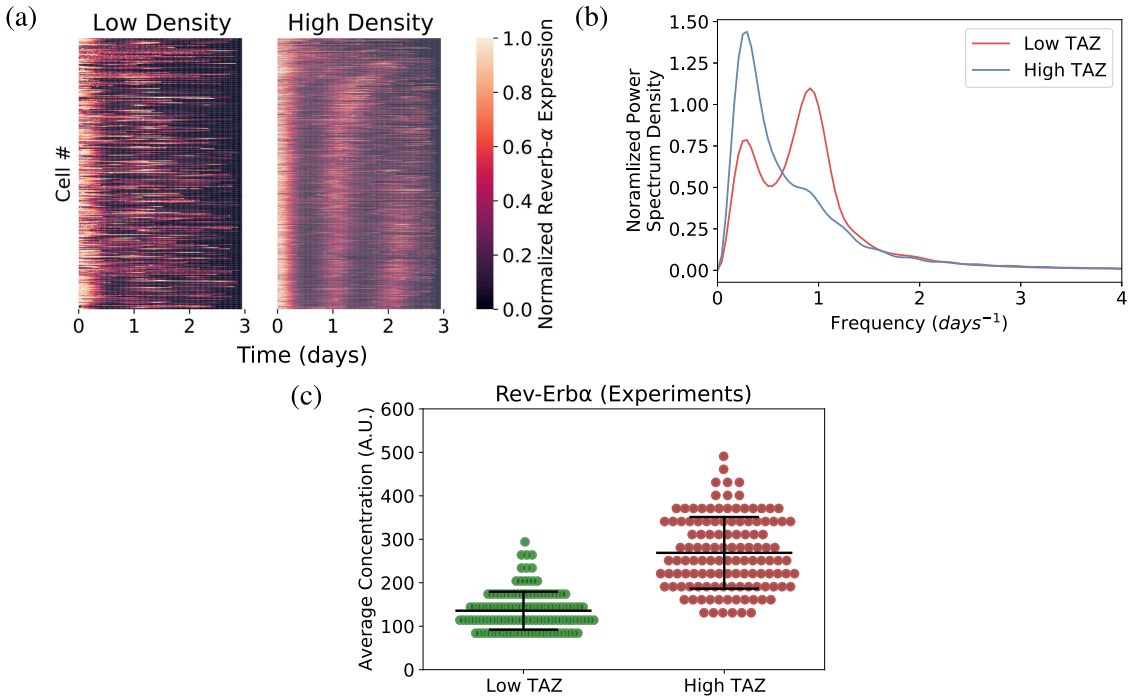


**FIG. 1.** Experimental results used to constrain our model. (a) Kymographs of Rev-Erbα expression in low (left) and high (right) densities mouse fibroblasts in *in vitro*. Each experiment lasted 72 h, and a total of 300 time points were sampled. The horizontal traces correspond to single cells and are ordered vertically by increasing amplitude of their circadian frequency. (b) Averaged Fourier spectra for two different levels of TAZ expression. (c) Effect of TAZ levels on Rev-Erbα expression. Data adapted from Abenza *et al.*[21]

of how large the oscillations are with respect to the average concentration values. Figure S1 in the supplementary material shows a comparison between the dynamics of the standard Goodwin model and our version, extended to account for saturation in the decay term of Rev-Erbα protein. In the absence of saturation (linear decay, standard case) the time trace for $Z$ has a very high mean value and, thus, a low modulation depth. Adding a nonlinearity in the decay term of $Z$ fixes this issue. Other additional nonlinearities, such as a nonlinear transcriptional activation of Rev-Erbα mRNA by Bmal1, have a similar effect, but the effect was larger for the $Z$ decay term in our case. Incidentally, the addition of an extra nonlinearity allowed us to lower the Hill coefficient $h$ from 11 to 2 with respect to the original parameters,[27] see Table I.

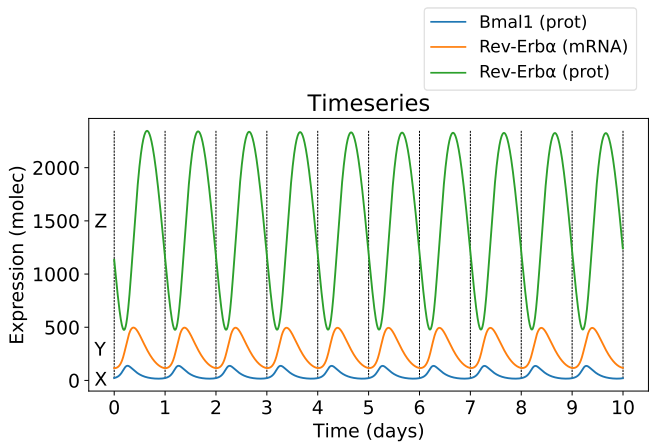


**FIG. 2.** Sample time series for the deterministic model with added saturation. Parameters are those given in Table I.

**TABLE I.** Parameter values used for the deterministic and stochastic simulations.

| Function | Parameter | Value | Units |
|---|---|---|---|
| Maximum Bmal expression | $\alpha_1$ | 5500 | molec·h$^{-1}$ |
| Production | $\beta_2$ | 1.3 | h$^{-1}$ |
| | $\beta_3$ | 1.3 | h$^{-1}$ |
| Degradation | $d_1$ | 0.26 | h$^{-1}$ |
| | $d_2$ | 0.26 | h$^{-1}$ |
| | $d_3$ | 3.9 | h$^{-1}$ |
| Hill coefficient | $h$ | 2 | … |
| Negative feedback threshold | $K$ | 50 | molec |
| Saturation | $S$ | 100 | molec |

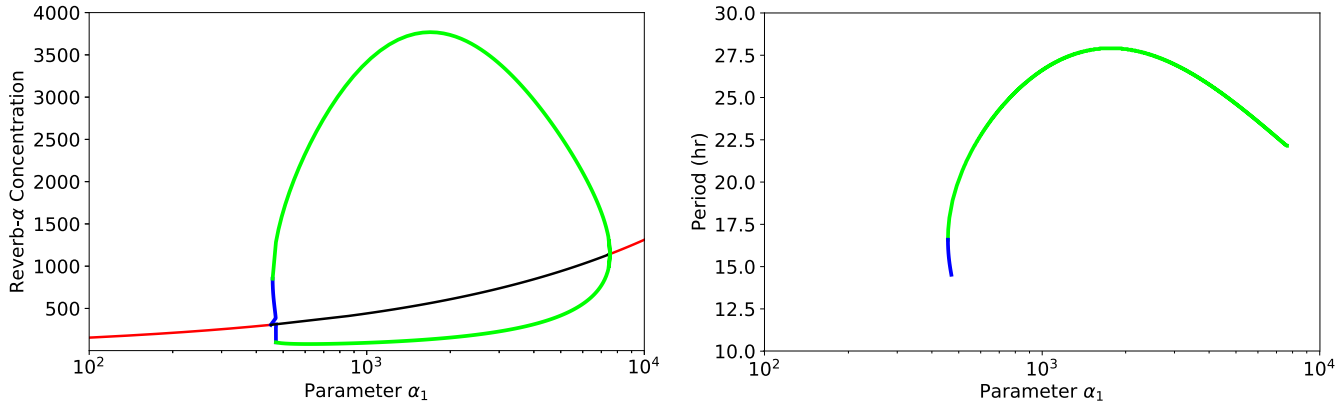


**FIG. 3.** Bifurcation diagram of the extended Goodwin model with saturation. Effect of changing the negative feedback parameter $\alpha_1$ on the concentration of Rev-Erbα (left) and the period (right). Red (black) lines indicate a stable (unstable) equilibrium, and green (blue) lines denote a stable (unstable) limit cycle. The maximum period occurs at the same point as the maximum amplitude. The system cycles with a period of 24 h for $\alpha_1 = 5500$ molec·h$^{-1}$, and this value is used as the base for the model below.

As mentioned above, experiments show that Rev-Erbα levels increase in concentration with TAZ expression [Fig. 1(c)],[21] both in its mean and standard deviation. The model, therefore, needs a way to introduce YAP/TAZ (and thus cell density) that leads to a comparable effect. On the basis of previous experimental evidence suggesting that YAP/TAZ affects the clock protein Bmal,[29–33] we chose to represent the effect of YAP/TAZ in the clock parametrically through modulation of the maximum Bmal expression rate $\alpha_1$, considering that an increase in $\alpha_1$ corresponds to a larger effect of YAP/TAZ on Bmal (and correspondingly to a lower cell density). As we show in what follows, increasing $\alpha_1$ disrupts the oscillations seen in the system and increases the average concentration of Rev-Erbα.[21]

To establish how the nature of the oscillations changes with $\alpha_1$, we use bifurcation analysis. The results of this analysis, performed with XPPAUT[34] and shown in Fig. 3, reveal that the system undergoes two Hopf bifurcations, one subcritical at $\alpha_1 \sim 470$ molec·h$^{-1}$ and the other supercritical at $\alpha_1 \sim 7500$ molec·h$^{-1}$. At the subcritical point, the system changes from settling to a stable steady state to undergo oscillations. At the supercritical point, the reverse occurs: the system stops oscillating and returns to a stable steady state. The amplitude varies within the region of oscillations, reaching a maximum of around 1800 molecules at $\alpha_1 \sim 1700$ molec·h$^{-1}$ and steadily decreasing until reaching the upper Hopf point. The period varies somewhat, with a minimum of $\sim 17$ h at the lower Hopf point, rapidly increasing to a maximum value of $\sim 27$ h at $\alpha_1 \sim 1700$ molec·h$^{-1}$ and then steadily decreasing to $\sim 22$ h at the upper Hopf point.

It is also worth pointing out that according to the bifurcation analysis results shown in Fig. 3, the fixed point of the system increases monotonically with $\alpha_1$ (both when stable and when unstable). This fact, together with the behavior of the extrema of the limit cycle itself, allow us to infer that the average Rev-Erbα levels increase monotonically with YAP/TAZ levels, in agreement with the experimental observation [Fig. 1(c)].

## IV. STOCHASTIC MODELING

Deterministic simulations were run first, as described above, to determine the proper values for parameters and establish a reasonable scale for molecule numbers. They provide a good starting point for the model and allow us to make qualitative inferences about the system. However, they lack the noise seen in true biological systems since the same time series is always produced from a given initial condition. Stochastic simulations more accurately capture biological processes through the addition of randomness. The next reaction method, a type of stochastic simulation, was used to simulate the circadian system, as implemented in the Python package `StochPy`.[35] The next reaction method considers each process in the system as a separate biochemical reaction that has a certain likelihood to occur, determined by its respective propensity.[36] In our case, the reactions are either the creation or degradation of one of the components of system, and the propensities for each are calculated using the same parameters from the deterministic model. A limitation of using the next reaction method to model biochemical reaction systems relates to the number of molecules present. In our model, we considered realistic Bmal and Rev-Erbα concentrations, with Rev-Erbα having 1000 molecules on average and Bmal having a maximum of around 100 molecules, for which the next-reaction method has an acceptable efficiency.[36,37]

### A. Ensembles of stochastic simulations

Two groups of stochastic simulations are run, reflecting different concentrations of YAP/TAZ: low ($\alpha_1 = 5500$ molec·h$^{-1}$) and high ($\alpha_1 = 10^6$ molec·h$^{-1}$). We recall that the level of YAP/TAZ is inversely related to cell density, where high cell density corresponds to low YAP/TAZ concentrations and vice versa. For each case, 1000 simulations are run for 20 days, using the corresponding value of $\alpha_1$. The remaining parameters are varied randomly with each simulation, adding an extra layer of noise to the system. Specifically, the parameters are selected from a log-normal distribution, centered

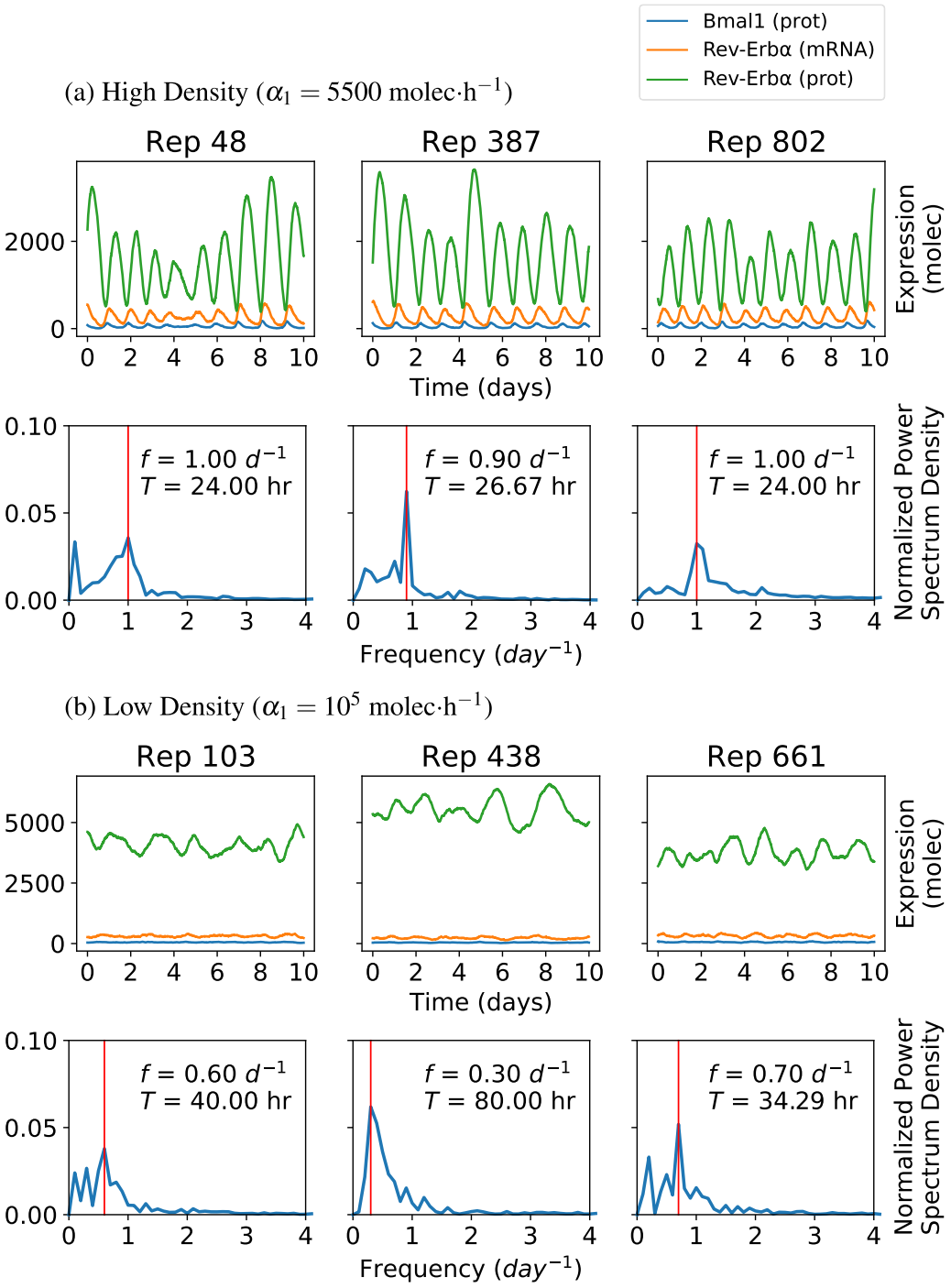


**FIG. 4.** Sample time series and Fourier spectra from the stochastic simulations. Three samples from the 1000 repetitions are shown for each of the high and low density cases. (a) High density ($\alpha_1 = 5500$ molec·h$^{-1}$); (b) low density ($\alpha_1 = 10^5$ molec·h$^{-1}$).

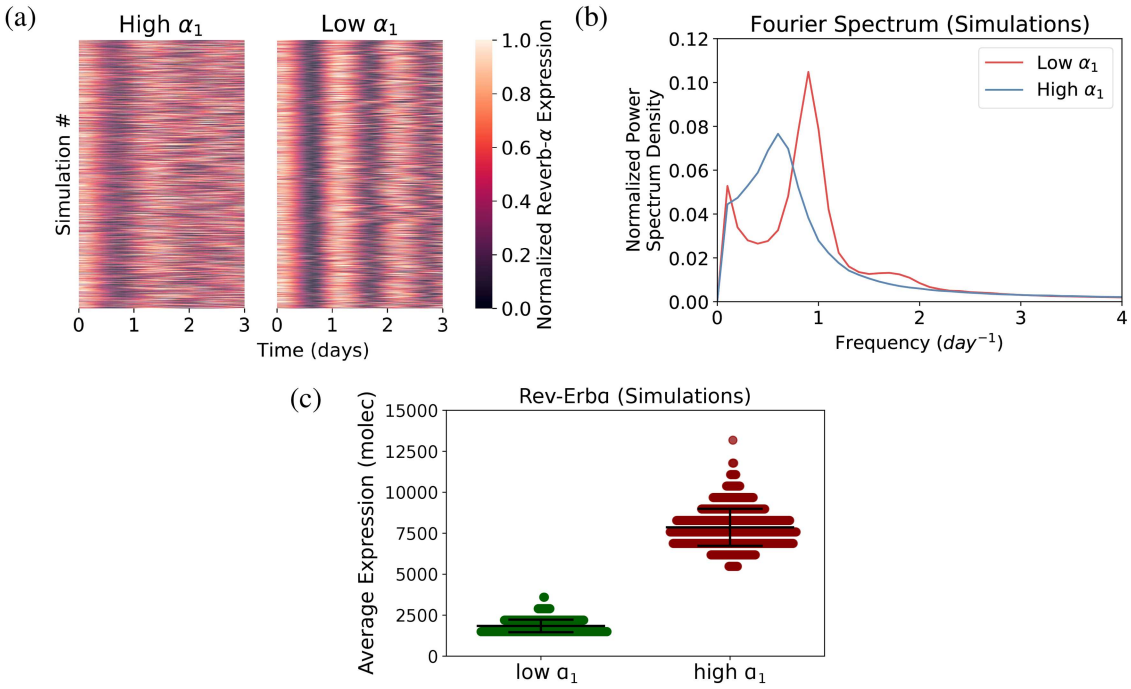


**FIG. 5.** (a) Kymograph of time series obtained with the stochastic simulations. Results are shown for both low ($\alpha_1 = 5500$ molec·h$^{-1}$) and high ($\alpha_1 = 10^5$ molec·h$^{-1}$) values of maximum Bmal expression, corresponding to high and low cell densities as shown in the experiments of Fig. 1(a). As in that figure, the horizontal traces (1000 in each case) are ordered vertically by increasing the amplitude of their circadian frequency. The time series are shown after a transient period and are aligned by their first peak in expression. A qualitative agreement is seen with Fig. 1(b). (b) Fourier spectrum averaged over 1000 stochastic simulations for the two values of $\alpha_1$ given above. The averages were taken over 1000 stochastic simulations each. (c) Effect of YAP/TAZ concentration on average concentration of Rev-Erbα in the stochastic simulations. Again, a qualitative agreement is seen with Fig. 1(c).

around the deterministic parameter values from Table I, and with a spread that is roughly 20% the parameter mean.

### B. Stochastic time series

The stochastic time series, examples of which are shown in Fig. 4, display steady oscillations for the case of low YAP/TAZ (high cell density), with a period around 24 h on average. The amplitude varies greatly between cycles of a given time series, but the period remains fairly consistent. For high YAP/TAZ (low cell density), the period was higher than 24 h for most of the simulations. Both the amplitude and period change from cycle to cycle, and the modulation depth is much lower compared to the high cell density case. Kymographs of the time series are shown in Fig. 5(a). Now that noise has been added to the system, the model better reflects the results seen in our reference experiments.[21]

### C. Fourier analysis

Fourier spectra were calculated and averaged over the 1000 simulations described above, for each of the two $\alpha_1$ values [Fig. 5(b)]. When $\alpha_1 = 5500$ molec·h$^{-1}$ (low YAP/TAZ, high cell density), the stochastic simulations have a dominant frequency centered at roughly 0.9 day$^{-1}$ (26.7 h), which disappears when the parameter $\alpha_1$ is increased to $10^5$ molec·h$^{-1}$. These results are consistent with the experimental observations shown in Fig. 1 above. Although the match is not perfect, the model produces the same qualitative behavior, as circadian robustness is lost in both cases with higher YAP/TAZ concentrations.

### D. Effect on circadian gene levels

As discussed briefly in Sec. III above, in our deterministic model, the average concentration of Rev-Erbα increases with $\alpha_1$. The stochastic simulations show that not only does the concentration increase but also becomes more variable across the simulations. This is shown in Fig. 5(c), which plots the instantaneous levels of Rev-Erbα obtained in our simulations for both low and high YAP/TAZ levels. These results fit with our experimental observations, where higher concentrations of TAZ correspond to higher Rev-Erbα concentrations with greater spread [Fig. 1(c)].[21]

The response of Rev-Erbα to a continuous increase in $\alpha_1$ is shown in Fig. 6, ranging from $\alpha_1 = 500$ molec·h$^{-1}$ to $10^5$ molec·h$^{-1}$, with steps of 50 molec·h$^{-1}$. For each value of $\alpha_1$, 10 simulations were run for 10 days. This allows us to see the behavior of the model throughout the entire range of YAP/TAZ levels. As the parameter $\alpha_1$ increases sufficiently, the expression of Rev-Erbα increases overall. For small values of $\alpha_1$ (less than $2 \times 10^4$ molec·h$^{-1}$), the average concentration increases first and then decreases, as $\alpha_1$ passes

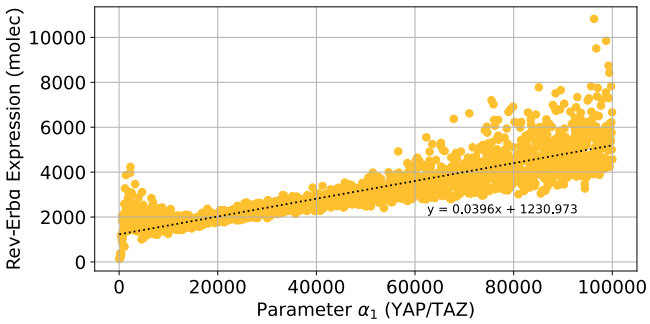


**FIG. 6.** Effect of a continuous increase in $\alpha_1$ on Rev-Erb$\alpha$ levels.

through and exits the oscillatory region. After this, the concentration steadily increases. Additionally, the average expression becomes more variable the further $\alpha_1$ is increased.

The results shown in Fig. 6 do not take into account the time structure of the system. For completeness, Fig. 7 shows how the time series behave as $\alpha_1$ increases continuously. The results show that circadian oscillations persist beyond the regime of deterministic limit cycle oscillations.[38] The relationship between increasing $\alpha_1$ and the variability in both amplitude and period was studied as well. In the deterministic model, as we showed in Fig. 3, the supercritical Hopf bifurcation at the right of the oscillatory domain occurs at $\alpha_1 \sim 7500\,\text{molec} \cdot \text{h}^{-1}$. In the stochastic model, as we now show in Fig. 8, the variability increases for both amplitude and period (see also Figs. 6 and 7). Unlike the deterministic model, however, in the stochastic model, the oscillations never truly disappear after the second Hopf bifurcation, although they do lose their circadian behavior of regular 24 h periods and stable amplitude. The fluctuations seen for these high values of $\alpha_1$ are, thus, driven by noise rather than by the oscillatory nature of the model itself.

## V. COMPARISON TO EXISTING MODELS INCLUDING THE PER/CRY LOOP

Previous models of circadian gene expression have been created to include both the Per/Cry and Bmal/Rev-Erb$\alpha$ loops.[22,39] We introduced the effect of YAP/TAZ on those models by modifying the production term of Bmal. Specifically, the study by Relógio *et al.*[22] introduces a model of 19 equations that describes the dynamics of the genes Per, Cry, Clock, Bmal, Rev-Erb, and Ror. The model not only considers the concentration of mRNA for each gene but also the concentrations of their respective proteins in the cytoplasm and nucleus. Equation (8) from the article gives the rate of change for concentrations of Bmal mRNA (called $y_5$). We varied the transcription rate $V_{5\,\text{max}}$ of the production term, which is controlled by concentrations of nuclear Rev-Erb and Ror protein.

The model of Almeida *et al.*,[39] in turn, focuses on the genes Per, Cry, Clock, Bmal, Rev-Erb, Dbp, E4BP4, and Ror, and introduces the clock controlled elements E-box, R-box, and D-box. The system contains eight equations and does not consider differences between concentrations in the cytoplasm and nucleus. In Eq. (4) from the article, we varied the production term of Bmal by adjusting the strength of the activation from $R_{box}$.

The results for models can be seen in Fig. 9. In both cases, bifurcations were seen when increasing the respective parameters that control the production of Bmal mRNA. This agrees qualitatively with the results in our model, although the modulation depth changes with $\alpha_1$ more strongly than in our case. The behavior of the period, on the other hand, differs notably from our case. Specifically, while the model of Relogio *et al.* exhibits a substantial robustness in the period to changes in $\alpha_1$, the model of Almeida *et al.* displays a strong dependence of the period on $\alpha_1$, with values that never reach 24 hr for the parameters chosen.

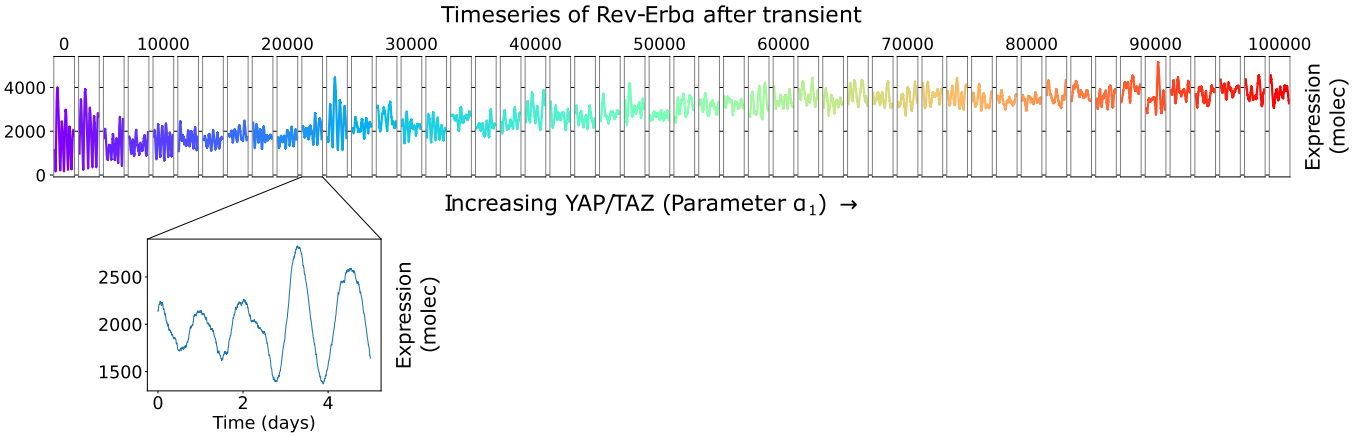


**FIG. 7.** Stochastic trajectories as parameter $\alpha_1$ is increased. Each window shows a distinct time series with its own set of parameters. All model parameters, except for the Hill coefficient $h$, are chosen from a log-normal distribution with a coefficient of 0.5 (as measured from the standard deviation and mean of the underlying normal distribution in each case. The distributions are centered around the deterministic parameter values, and the standard deviation was adjusted to introduce greater variability.

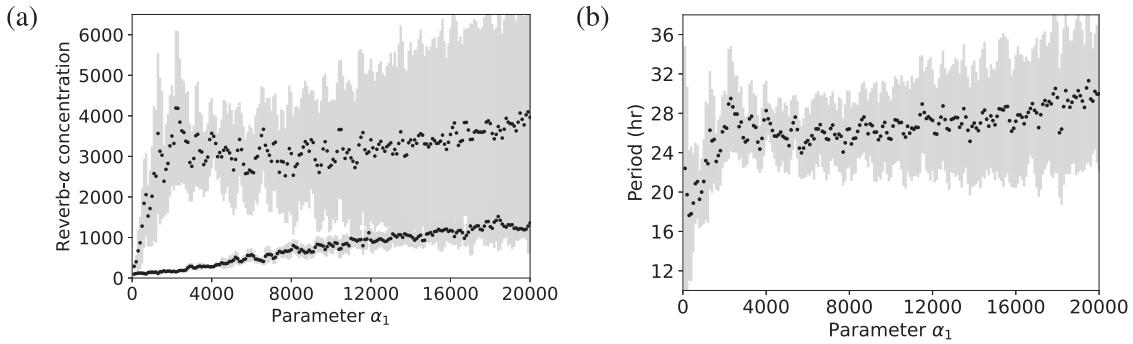


**FIG. 8.** Variability in the oscillations of the stochastic model as a function of $\alpha_1$. Changes in Rev-Erb$\alpha$ concentration (a) and period (b) are shown. The black dots represent the average minimum and maximum points of the oscillations (a) and their average period (b). The gray bars show the standard deviation of these values.

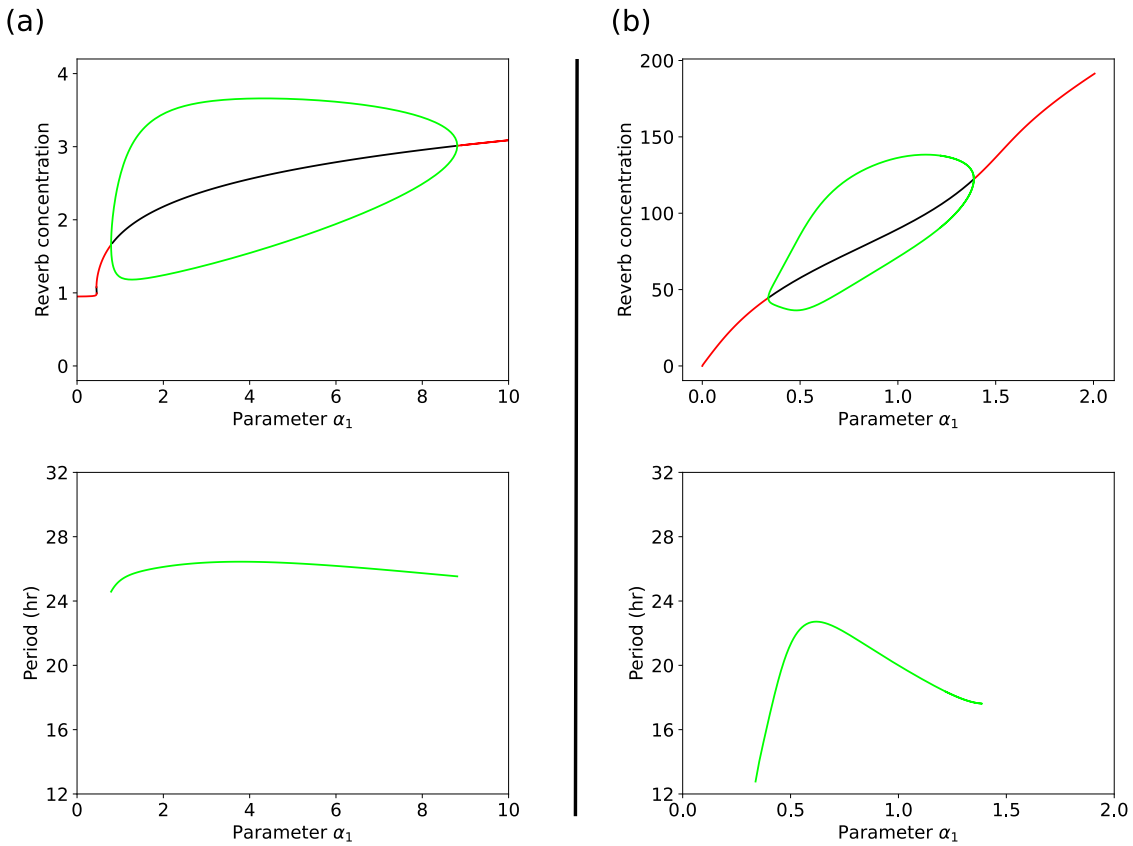


**FIG. 9.** Bifurcation analysis of models including the Per–Cry loop. (a) Model from Relogio *et al.*[22] As parameter $\alpha_1$ we chose their parameter $V_{5\,max}$, the maximum transcription rate of Bmal. (b) Model from Almeida *et al.*[39] The parameter $\alpha_1$ used here is a scaling factor multiplying the concentration of Ror in the equation for Bmal.

## VI. DISCUSSION

Here, we used a modified version of the Goodwin model to simulate a circadian clock. The effect of the mechanotransducer YAP/TAZ on the robustness of the clock was incorporated by varying the parameter associated with Bmal expression. Overall, the results from the model are consistent with experimental results.[21] As the concentration of YAP/TAZ increased, the average concentration of Rev-Erbα increased as well. Overall, the results of the model support the idea that YAP/TAZ concentrations affect the circadian behavior of mammalian cells via its connection to Bmal. The model also predicts that circadian oscillations would be lost for low values of $\alpha_1$, corresponding to cell densities higher than the basal values considered in the experiments shown in Fig. 1. It is also worth mentioning that the model predicts a positive correlation between the amplitude and period of circadian oscillations, as shown in Fig. 3. This correlation, known as twist, has been observed in other models,[40] where it has an impact on the entrainment and synchronization capabilities of the clock.

Our study required us to modify the original Goodwin model. Although the standard version of this model (in which all decay terms are linear) indeed describes an oscillatory system, it fails to capture all of the aspects of the experiments. The principal issue of the standard model is that the oscillations continue to be present for increasing values of $\alpha_1$. Additionally, the period of the oscillations stays fixed at 24 h no matter how high $\alpha_1$ is raised. Another issue with the standard Goodwin model is the modulation depth of the time series, defined as the amplitude of the oscillations divided by their mean, which provides an idea of how substantial the oscillations are with respect to the average concentration values. Here, we have shown that these issues can be addressed by changing the linear degradation term for Rev-Erbα protein to include a saturation term [Eq. (3)]. Notably, this also allows for a much smaller Hill coefficient $h$ in the negative feedback term of $X$ by $Z$,[41] which can now be decreased from 11 to 2.

There are other ways in which the experimental results of Fig. 1 could be reproduced with our model. Specifically, a dimensional analysis shows that the model could be rewritten in terms of a smaller number of free parameters as

$$\frac{dX'}{dt'} = \frac{\alpha_1'}{1+Z^h} - X, \tag{4}$$

$$\frac{dY'}{dt'} = X - d_2' Y, \tag{5}$$

$$\frac{dZ'}{dt'} = Y - \frac{d_3' Z}{1+Z/S'}, \tag{6}$$

where all variables and parameters are now dimensionless. In particular, $\alpha_1' = \alpha_1\beta_2\beta_3/(Kd_1^3)$. This indicates that the increase in $\alpha_1$ studied above can be recapitulated by an increase in $\beta_2$ and/or in $\beta_3$ and/or a decrease in $K$. This can be seen in Fig. 2 in the supplementary material, which shows how varying those four parameters leads to similar effects on the oscillations, from the point of view of both their existence and period. Therefore, our analysis cannot discern between the different parts of the Rev-Erbα transcription-translation feedback loop, in terms of where in the loop YAP/TAZ acts. Nevertheless, it does show that interfering with this negative feedback loop recapitulates the experimental observations. Here, we chose to interpret our results in terms of mechanical effects on Bmal, on the basis of the above-mentioned experimental observations that YAP/TAZ influences that clock protein.[29–33]

Further work could be done to consider how cells behave in proximity to other cells through the use of agent-based modeling to model mechanical effects among fibroblasts. Each cell would contain its own circadian model, regulating the concentrations of Bmal and Rev-Erbα. Changes in the cellular environment (high or low cell density) would drive changes in the parameter $\alpha_1$. This could easily be adapted to respond to other mechanical inputs into the cell, potentially shedding further light on the interplay between the mechanical and biochemical regulation of cellular dynamics.

## SUPPLEMENTARY MATERIAL

See figures in the supplementary material for the effect of the nonlinear degradation of $Z$ on the dynamics of the Goodwin model and the influence of other model parameters besides $\alpha_1$ ($K_1$, $\beta_2$, and $\beta_3$) on the bifurcations described in the paper.

## ACKNOWLEDGMENTS

This work was supported by Project Nos. PID2021-127311NB-I00 and PGC2018-099645-B-I00, financed by the Spanish Ministry of Science and Innovation, the Spanish State Research Agency, and FEDER (MICIN/AEI/10.13039/501100011033/FEDER), by the Maria de Maeztu Programme for Units of Excellence in R&D (Project No. CEX2018-000792-M), and by the Generalitat de Catalunya (ICREA Academia programme). Additional funding was provided by the Generalitat de Catalunya (AGAUR 2021 SGR 01425 and 2021 SGR 00175, and the CERCA Programme), and the European Research Council (Adv-883739). IBEC is a recipient of a Severo Ochoa Award of Excellence from the Ministry for Science and Innovation.

## AUTHOR DECLARATIONS

### Conflict of Interest

The authors have no conflicts to disclose.

### Author Contributions

**Keith E. Kennedy:** Conceptualization (equal); Formal analysis (equal); Investigation (equal); Methodology (equal); Software (equal); Validation (equal); Visualization (equal); Writing – original draft (equal). **Juan F. Abenza:** Conceptualization (equal); Data curation (equal); Investigation (equal); Resources (equal); Writing – review & editing (equal). **Leone Rossetti:** Conceptualization (equal); Data curation (equal); Investigation (equal); Resources (equal); Writing – review & editing (equal). **Xavier Trepat:** Conceptualization (equal); Investigation (equal); Methodology (equal); Resources (equal); Supervision (equal); Writing – review & editing (equal). **Pablo Villoslada:** Conceptualization (equal); Investigation (equal); Supervision (equal); Writing – review & editing (equal).

**Jordi Garcia-Ojalvo:** Conceptualization (equal); Funding acquisition (equal); Investigation (equal); Project administration (equal); Supervision (equal); Writing – original draft (equal).

## DATA AVAILABILITY

The data that support the findings of this study are available from the corresponding author upon reasonable request.

## REFERENCES


[1] A. Goldbeter, *Biochemical Oscillations and Cellular Rhythms* (Cambridge University Press, 1996).
[2] M. H. Hastings, A. B. Reddy, and E. S. Maywood, "A clockwork web: Circadian timing in brain and periphery, in health and disease," Nat. Rev. Neurosci. **4**, 649–661 (2003).
[3] J. S. Takahashi, "Transcriptional architecture of the mammalian circadian clock," Nat. Rev. Genet. **18**, 164–179 (2017).
[4] N. Kronfeld-Schor and T. Dayan, "Partitioning of time as an ecological resource," Annu. Rev. Ecol. Evol. Syst. **34**, 153–181 (2003).
[5] S. Yamaguchi, H. Isejima, T. Matsuo, R. Okura, K. Yagita, M. Kobayashi, and H. Okamura, "Synchronization of cellular clocks in the suprachiasmatic nucleus," Science **302**, 1408–1412 (2003).
[6] J. A. Mohawk, C. B. Green, and J. S. Takahashi, "Central and peripheral circadian clocks in mammals," Annu. Rev. Neurosci. **35**, 445–462 (2012).
[7] A. T. Winfree, "Biological rhythms and the behavior of populations of coupled oscillators," J. Theoret. Biol. **16**, 1542 (1967).
[8] Y. Kuramoto, "Self-entrainment of a population of coupled non-linear oscillators," in *International Symposium on Mathematical Problems in Theoretical Physics*, edited by H. Araki (Springer, Berlin, 1975), pp. 420–422.
[9] N. Kopell and G. Ermentrout, "Coupled oscillators and the design of central pattern generators," Math. Biosci. **90**, 87–109 (1988).
[10] A. Pikovsky, M. Rosenblum, and J. Kurths, *Synchronization: A Universal Concept in Nonlinear Sciences* (Cambridge University Press, 2001).
[11] S. Boccaletti, J. Kurths, G. Osipov, D. Valladares, and C. Zhou, "The synchronization of chaotic systems," Phys. Rep. **366**, 1–101 (2002).
[12] A. Arenas, A. Díaz-Guilera, J. Kurths, Y. Moreno, and C. Zhou, "Synchronization in complex networks," Phys. Rep. **469**, 93–153 (2008).
[13] H. R. Ueda, K. Hirose, and M. Iino, "Intercellular coupling mechanism for synchronized and noise-resistant circadian oscillators," J. Theor. Biol. **216**, 501–512 (2002).
[14] D. Gonze, S. Bernard, C. Waltermann, A. Kramer, and H. Herzel, "Spontaneous synchronization of coupled circadian oscillators," Biophys. J. **89**, 120–129 (2005).
[15] S. Bernard, D. Gonze, B. Čajavec, H. Herzel, and A. Kramer, "Synchronization-induced rhythmicity of circadian oscillators in the suprachiasmatic nucleus," PLoS Comput. Biol. **3**, e68 (2007).
[16] T.-L. To, M. A. Henson, E. D. Herzog, and F. J. Doyle, "A molecular model for intercellular synchronization in the mammalian circadian clock," Biophys. J. **92**, 3792–3803 (2007).
[17] U. Abraham, A. E. Granada, P. O. Westermark, M. Heine, A. Kramer, and H. Herzel, "Coupling governs entrainment range of circadian clocks," Mol. Syst. Biol. **6**, 438 (2010).
[18] O. Burckard, M. Teboul, F. Delaunay, and M. Chaves, "Cycle dynamics and synchronization in a coupled network of peripheral circadian clocks," Interface Focus **12**, 20210087 (2022).
[19] S. Dupont, L. Morsut, M. Aragona, E. Enzo, S. Giulitti, M. Cordenonsi, F. Zanconato, J. Le Digabel, M. Forcato, S. Bicciato, N. Elvassore, and S. Piccolo, "Role of YAP/TAZ in mechanotransduction," Nature **474**, 179–184 (2011).
[20] I. G. Macara, "Transport into and out of the nucleus," Microbiol. Mol. Biol. Rev. **65**, 570–594 (2001).
[21] J. F. Abenza, L. Rossetti, M. Mouelhi, J. Burgués, I. Andreu, K. Kennedy, P. Roca-Cusachs, S. Marco, J. García-Ojalvo, and X. Trepat, "Mechanical control of the mammalian circadian clock via YAP/TAZ and TEAD," bioRxiv (2022), https://doi.org/10.1101/2022.02.04.478830
[22] A. Relógio, P. O. Westermark, T. Wallach, K. Schellenberg, A. Kramer, and H. Herzel, "Tuning the mammalian circadian clock: Robust synergy of two loops," PLoS Comput. Biol. **7**, e1002309 (2011).
[23] H. Cho, X. Zhao, M. Hatori, R. T. Yu, G. D. Barish, M. T. Lam, L. W. Chong, L. Ditacchio, A. R. Atkins, C. K. Glass, C. Liddle, J. Auwerx, M. Downes, S. Panda, and R. M. Evans, "Regulation of circadian behaviour and metabolism by REV-ERB-$\alpha$ and REV-ERB-$\beta$," Nature **485**, 123–127 (2012).
[24] C. Hsiao, M. Lampe, S. Nillasithanukroh, W. Han, X. Lian, and S. P. Palecek, "Human pluripotent stem cell culture density modulates YAP signaling," Biotechnol. J. **11**, 662–675 (2016).
[25] B. C. Goodwin, "Oscillatory behavior in enzymatic control processes," Adv. Enzym. Regul. **3**, 425–437 (1965).
[26] E. Ullner, J. Buceta, A. Díez-Noguera, and J. García-Ojalvo, "Noise-induced coherence in multicellular circadian clocks," Biophys. J. **96**, 3573–3581 (2009).
[27] B. Ananthasubramaniam, C. Schmal, and H. Herzel, "Amplitude effects allow short jet lags and large seasonal phase shifts in minimal clock models," J. Mol. Biol. **432**, 3722–3737 (2020).
[28] R. Milo, R. Phillips, and N. Orme, *Cell Biology by the Numbers* (Garland Science, 2008).
[29] B. Zhao, X. Ye, J. Yu, L. Li, W. Li, S. Li, J. Yu, J. D. Lin, C. Y. Wang, A. M. Chinnaiyan, Z. C. Lai, and K. L. Guan, "TEAD mediates YAP-dependent gene induction and growth control," Genes Dev. **22**, 1962–1971 (2008).
[30] F. Zanconato, M. Forcato, G. Battilana, L. Azzolin, E. Quaranta, B. Bodega, A. Rosato, S. Bicciato, M. Cordenonsi, and S. Piccolo, "Genome-wide association between YAP/TAZ/TEAD and AP-1 at enhancers drives oncogenic growth," Nat. Cell. Biol. **17**, 1218–1227 (2015).
[31] D. H. Lee, J. O. Park, T. S. Kim, S. K. Kim, T. H. Kim, M. C. Kim, G. S. Park, J. H. Kim, S. Kuninaka, E. N. Olson, H. Saya, S. Y. Kim, H. Lee, and D. S. Lim, "LATS-YAP/TAZ controls lineage specification by regulating TGF$\beta$ signaling and Hnf4$\alpha$ expression during liver development," Nat. Commun. **7**, 11961 (2016).
[32] A. Rivera-Reyes *et al.*, "YAP1 enhances NF-$\kappa$B-dependent and independent effects on clock-mediated unfolded protein responses and autophagy in sarcoma," Cell Death Dis. **9**, 1108 (2018).
[33] P. Rajbhandari *et al.*, "Cross-cohort analysis identifies a TEAD4-MYCN positive-feedback loop as the core regulatory element of high-risk neuroblastoma," Cancer Discov. **8**, 582–599 (2018).
[34] B. Ermentrout, *Simulating, Analyzing, and Animating Dynamical Systems: A Guide to XPPAUT for Researchers and Students* (Society for Industrial and Applied Mathematics, 2002).
[35] T. R. Maarleveld, B. G. Olivier, and F. J. Bruggeman, "StochPy: A comprehensive, user-friendly tool for simulating stochastic biological processes," PLoS One **8**, e79345 (2013).
[36] D. T. Gillespie, "Stochastic simulation of chemical kinetics," Annu. Rev. Phys. Chem. **58**, 35–55 (2007).
[37] F. Y. Rodríguez and A. P. Muñuzuri, "A goodwin model modification and its interactions in complex networks," Entropy **25**, 894 (2023).
[38] A. Neiman, P. I. Saparin, and L. Stone, "Coherence resonance at noisy precursors of bifurcations in nonlinear dynamical systems," Phys. Rev. E **56**, 270–273 (1997).
[39] S. Almeida, M. Chaves, and F. Delaunay, "Transcription-based circadian mechanism controls the duration of molecular clock states in response to signaling inputs," J. Theor. Biol. **484**, 110015 (2020).
[40] M. del Olmo, C. Schmal, C. Mizaikoff, S. Grabe, C. Gabriel, A. Kramer, and H. Herzel, "Are circadian amplitudes and periods correlated? a new twist in the story," bioRxiv (2023), doi:10.1101/2023.05.17.541139
[41] J. D. Murray, *Mathematical Biology. I. An Introduction*, 3rd ed. (Springer, 2002).